Effects of Cu alloying on the structural and electronic properties in amorphous $Cu_x(As_{0.4}S_{0.6})_{1-x}$: *Ab initio* molecular-dynamics simulations

Fuyuki Shimojo and Masaru Aniya
Department of Physics, Kumamoto University, Kumamoto 860-8555, Japan
(Received 3 April 2006; published 23 June 2006)

The composition dependence of the atomic structure and bonding properties in amorphous $Cu_x(As_{0.4}S_{0.6})_{1-x}$ (x=0.0, 0.024, and 0.11) is investigated by means of *ab initio* molecular-dynamics simulations. Our results show that Cu atoms introduced tend to bind with S atoms with a well defined bond length. The pair distribution functions obtained reveal that As-As correlation is influenced appreciably by the addition of Cu atoms, whereas changes in S-S correlation are relatively small. It is found that the unoccupied electronic states near the bottom of the conduction band have a nonbonding character and have large amplitudes of their wave functions around the As atoms that are coordinated with two S atoms as well as around Cu atoms. We suggest that these electronic states will play an important role in the suppression of photodarkening in Cu-doped arsenic chalcogenides.

DOI: 10.1103/PhysRevB.73.235212 PACS number(s): 61.43.Dq, 71.23.Cq, 71.15.Pd

I. INTRODUCTION

Amorphous arsenic chalcogenides such as As_2S_3 and As_2Se_3 have a network structure of covalently bonded atoms. Arsenic and chalcogen atoms have basically threefold and twofold coordinations, respectively, and the heterocoordination is preferred.[1] While this short-range structure is similar to that of crystals, these amorphous materials exhibit physical properties, which are not seen in their crystalline phases, due to the disorderness and structural flexibility in medium-range and long-range structures.[2]

Under illumination amorphous chalcogenides show a wide variety of photoinduced phenomena such as photodarkening, photobleaching, photopolimerization, photodoping, photoinduced anisotropy, photoexpansion, etc.[3–7] Among these, considerable efforts have been made for many years to understand photodarkening,[8–10] which is a phenomenon of the shift of the optical absorption edge toward a longer wavelength after the illumination with near band gap light. X-ray diffraction studies have demonstrated that changes in the network structure due to illumination are responsible for photodarkening.[11] It is known that photodarkening is suppressed by the addition of a small amount (1–5%) of metals such as Cu,[12] Pb,[13] and Sn.[14] These observations indicate that the electronic properties of amorphous chalcogenides are closely related to the structure of atoms. However, in spite of considerable efforts over the past years, and the presentation of a wide range of proposed models, the precise nature of the mechanism that gives rise to these phenomena still remains elusive.[15] In order to clarify the microscopic mechanism, understanding of the fundamental materials properties is indispensable.

So far, several theoretical studies have been conducted on amorphous chalcogenides.[16–24] Li and Drabold have carried out molecular-dynamics (MD) simulations of amorphous As_2Se_3 based on a nonorthogonal tight binding scheme.[17] They investigated the local vibrational modes and the electronic density of states, as well as the structure of atoms and showed that their calculated results are consistent with experiments. They found that bond-breaking and bond-switching reactions occur around defect sites under illumination in metal-free amorphous As_2Se_3, and that there are two time scales in the relaxation processes of the network structure.[18] The structural properties of amorphous As_2S_3 have been investigated by *ab initio* MD simulations of Shimojo *et al.*[19] They reported on effects of hydrostatic compression on the local atomic configuration. More recently, semiempirical tight-binding calculations have been carried out for amorphous As_2S_3 by Elliott and co-workers.[20–22] They suggested that there exist defect pairs, $[As_4]^-$-$[S_3]^+$, in addition to the charged coordination defects, and that such defect pairs are responsible for photodarkening under illumination. They also studied the influence of alloying Cu on the electronic properties and discussed the mechanism of the suppression of photodarkening in Cu-doped chalcogenides. Singh and Oh have presented a quantum mechanical theory to study photoinduced phenomena in amorphous chalcogenides with considering the excited electrons.[23] We have suggested an agglomeration tendency of noble metals in amorphous metal-doped chalcogenides.[24]

It is known that, in metal-doped arsenic chalcogenides, the electrical conductivity increases largely accompanied with a reduction of the optical gap with increasing metal contents.[25] Since the conductivities are usually unresponsive to the presence of impurities in amorphous semiconductors, the unexpected increase in the conductivity is considered to arise from some substantial changes in the atomic structure,[26–28] which will affect photoinduced phenomena. However, details of the local structure around the impurity metals are still unknown.

In the present study, we investigate the composition dependence of the atomic structure, electronic structure and bonding properties in amorphous $Cu_x(As_{0.4}S_{0.6})_{1-x}$ (x=0.0, 0.024, and 0.11) by means of *ab initio* MD simulations. The main purpose of our research is to clarify the effects of Cu alloying on the structural and electronic properties in amorphous chalcogenides from first principles. We will discuss in detail how the network structure is modified by the addition of Cu atoms. The bonding properties of atoms are examined by the population analysis with respect to the local coordi-

nation of atoms. Also the electronic states near the band gap are investigated in connection with the suppression of photodarkening.

II. METHOD OF CALCULATION

In our *ab initio* MD simulations for amorphous $Cu_x(As_{0.4}S_{0.6})_{1-x}$, atomic forces were calculated from the electronic ground state within the generalized gradient approximation[29] to the density functional theory. The energy functional was minimized using an iterative scheme based on a preconditioned conjugate-gradient method.[30–32] We used ultrasoft pseudopotentials[33] with a plane-wave basis set. The Γ point was used to sample the Brillouin zone of supercells, and the plane-wave cutoff energies for the wave functions and the charge density are 20 and 150 Ry., respectively. Using the Nosé-Hoover thermostat technique, the equations of motion were solved via explicit reversible integrators.[34] The initial charge density at each MD step was estimated by extrapolating the charge densities at the previous steps,[32] and the initial wave functions were estimated from the wave functions at the previous steps by means of a subspace diagonalization.[31]

We used three systems composed of 80 atoms (32As+48S), 82 atoms (32As+48S+2Cu), and 90 atoms (32As+48S+10Cu) for the concentrations of $x=0.0$, 0.024, and 0.11, respectively, in cubic supercells under periodic boundary conditions. The system sizes were selected to be large enough for the current purpose of studying the local structure and bonding properties around Cu atoms. To obtain amorphous states, we began with carrying out a simulation up to 10 ps for a liquid state at 1000 K, and then decreased the temperature of the system gradually to 400 K with a decreasing rate of 20 K/ps. Since the starting temperature 1000 K is quite high compared with the melting temperature 585 K of As_2S_3, the system came into a disordered state without the effects of initial configuration. The amorphous state at 400 K was simulated for at least 11 ps. The number density of atoms 0.0381 $Å^{-3}$ was determined by the zero-pressure condition for simulations of As_2S_3 ($x=0.0$), which agrees well with the experimental value, 0.039 $Å^{-3}$.[1] Since it has been observed experimentally that the number density is almost unchanged for Cu concentrations up to about 10%,[28] we used the same number density for $x=0.024$ and 0.11 as that for $x=0.0$. The quantities of interest were obtained by averaging over more than 8 ps after the initial equilibration taking about 3 ps.

It would be valuable to discuss the possible inaccuracies of our computational method. First, the size of the system could be a problem, considering the fact that the number of atoms used in the previous studies based on tight binding schemes[17,18,20,22] is about 200. Since the edge length of our supercell is about 14 Å, we are unable to investigate the spatial correlation beyond half the edge length ~7 Å. In this paper, we focus only on atomic correlations within the distance of 7 Å, which is large enough to the purpose of our study. Second, the underestimation of the electronic energy gap at the Fermi level by the approximation[29] to the density functional theory could cause incorrect electronic properties.

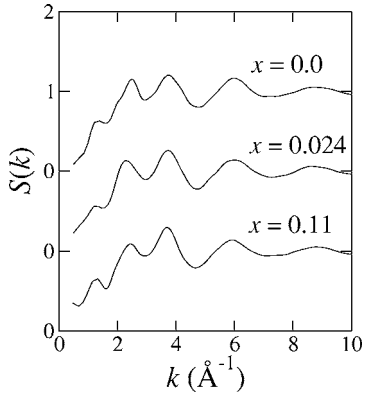

FIG. 1. Structure factors $S(k)$ of amorphous $Cu_x(As_{0.4}S_{0.6})_{1-x}$ obtained from the partial structure factors $S_{\alpha\beta}(k)$ using the neutron scattering lengths. Each curve was calculated using a Gaussian filter with a width of $\Delta k=0.1$ $Å^{-1}$ to eliminate statistical errors.

As will be shown by the calculated electronic density of states, the semiconducting properties are successfully reproduced by our models, and the concentration dependence of the energy gap is similar to that observed experimentally. We will give qualitative discussion on the electronic states near the Fermi level, although we cannot examine the energy gap quantitatively. Last, the limited length of simulation time could cause some statistical errors. Also the decreasing rate of temperature could be too fast to obtain an amorphous state. However, since the calculated structures are consistent with the experimental results, we think that the simulation time is long enough to reproduce and investigate the amorphous states.

III. RESULTS

A. Structure factors

The structure factors $S(k)$ calculated by our *ab initio* MD simulations are shown in Fig. 1. They were obtained from the partial structure factors $S_{\alpha\beta}(k)$, shown in Fig. 2, using the

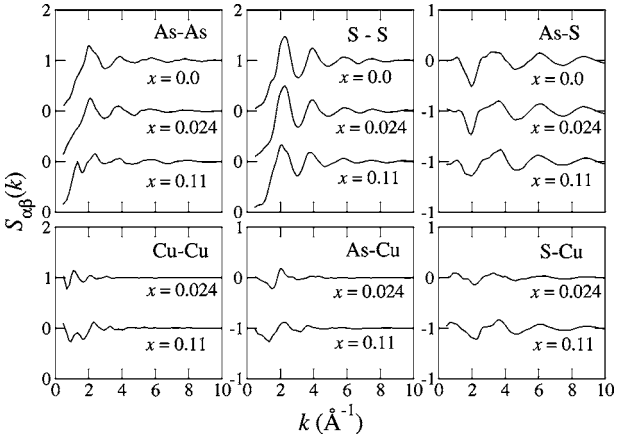

FIG. 2. Ashcroft-Langreth partial structure factors $S_{\alpha\beta}(k)$ of amorphous $Cu_x(As_{0.4}S_{0.6})_{1-x}$. Each curve was calculated using a Gaussian filter with a width of $\Delta k=0.1$ $Å^{-1}$ to eliminate statistical errors.

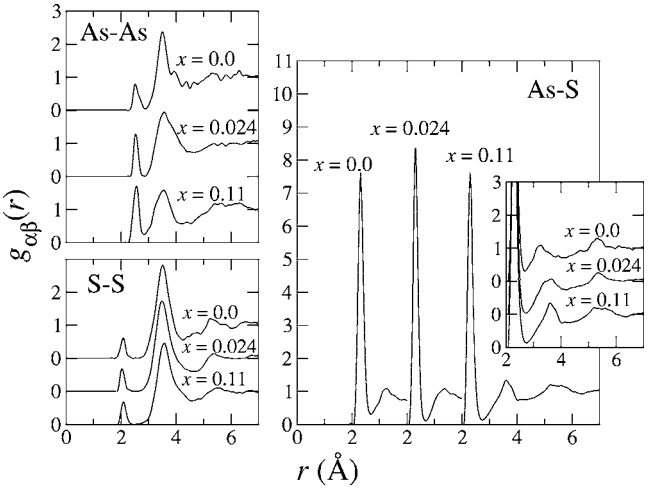

FIG. 3. Partial pair distribution functions $g_{\alpha\beta}(r)$ of amorphous $Cu_x(As_{0.4}S_{0.6})_{1-x}$ for $\alpha-\beta$=As-As, S-S, and As-S.

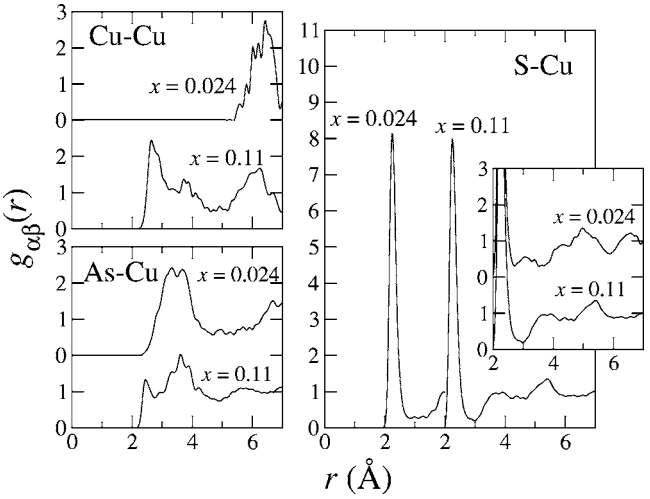

FIG. 4. Partial pair distribution functions $g_{\alpha\beta}(r)$ of amorphous $Cu_x(As_{0.4}S_{0.6})_{1-x}$ for $\alpha-\beta$=Cu-Cu, As-Cu, and S-Cu.

neutron scattering lengths. Note that the structure factors obtained by using the x-ray form factors are indistinguishable to $S(k)$ shown in Fig. 1. In $S(k)$ for As_2S_3 (x=0.0), there is a first-sharp diffraction peak (FSDP) at k=1.3 Å^{-1}. The first main peak appears at k=2.2 Å^{-1}, and the positions of the second and third peaks are at k=3.8 and 6.0 Å^{-1}, respectively. We see that an oscillating behavior in $S(k)$ remains for $k>10$ Å^{-1} (not shown in Fig. 1). These features are in agreement with the results of neutron scattering experiments.[1] The addition of Cu atoms does not change the overall profile of $S(k)$, although the second peak becomes higher with increasing concentration x.

It is worth while examining the calculated partial structure factors $S_{\alpha\beta}(k)$, since it is difficult to obtain those quantities for ternary compounds from experiments. Figure 2 shows the Ashcroft-Langreth partial structure factors $S_{\alpha\beta}(k)$. It is seen that $S_{\mathrm{AsAs}}(k)$ and $S_{\mathrm{SS}}(k)$ have main peaks at almost the same wave vectors (k=2.0–2.3 Å^{-1}), at which $S_{\mathrm{AsS}}(k)$ has a large dip. When the Cu concentration x is increased from 0.024 to 0.11, the peak at k=2.0 Å^{-1} in $S_{\mathrm{AsAs}}(k)$ shifts to a larger wave vector k=2.2 Å^{-1}, whereas $S_{\mathrm{SS}}(k)$ changes the position of its peak from k=2.2 Å^{-1} to a smaller wave vector k=2.0 Å^{-1}. We see that there is a shoulder at k=2.2 Å^{-1} in $S_{\mathrm{AsAs}}(k)$ for x=0.0 and 0.024, and in $S_{\mathrm{SS}}(k)$ for x=0.11. It should be noted that, in $S_{\mathrm{AsAs}}(k)$, a peak grows at k=1.3 Å^{-1}, at which the FSDP of $S(k)$ is seen. This means that the spatial correlation between As atoms changes in the scale of intermediate distance ~5 Å with increasing Cu concentration x. In $S_{\mathrm{CuCu}}(k)$ and $S_{\mathrm{AsCu}}(k)$, there are some structures only for $k<4.0$ Å^{-1}, which reflects the fact that the Cu concentration is rather low. However, in $S_{\mathrm{SCu}}(k)$ especially for x=0.11, an oscillating behavior continues to larger wave vectors, indicating that there exists a short-range correlation between Cu and S atoms.

B. Pair distribution functions

The partial pair distribution functions $g_{\alpha\beta}(r)$ for α-β=As-As, S-S, and As-S pairs are shown in Fig. 3. We can see clearly that the preferred bond is the heteropolar As-S bond among the three correlations, as $g_{\mathrm{AsS}}(r)$ has a large peak at r=2.3 Å. In $g_{\mathrm{AsAs}}(r)$ and $g_{\mathrm{SS}}(r)$, there are small peaks at r=2.6 and 2.1 Å, respectively, so a few homopolar As-As and S-S bonds exist in amorphous $Cu_x(As_{0.4}S_{0.6})_{1-x}$. Figure 4 shows $g_{\alpha\beta}(r)$ related to Cu atoms for x=0.024 and 0.11. We see that Cu atoms have a preference to bind with S atoms as reflected by a sharp peak in $g_{\mathrm{SCu}}(r)$ at r=2.3 Å. Figure 4 also indicates that there is a formation of As-Cu bonds when the Cu concentration reaches x=0.11 as displayed by a first small peak in $g_{\mathrm{AsCu}}(r)$ at r=2.5 Å. The finding that Cu atoms bind to S atoms as well as to As atoms is in agreement with x-ray photoelectron spectroscopy (XPS) measurement.[35] In $g_{\mathrm{CuCu}}(r)$ for x=0.11, a peak appears at r =2.8 Å, which indicates a possible aggregation tendency of Cu atoms as has been found in the disordered phases of CuI.[36]

The coordination number $N_{\alpha\beta}$, which is the average number of β-type atoms coordinated with an α-type atom, was calculated as

$$N_{\alpha\beta}=\rho_\beta\int_0^{R_{\alpha\beta}}4\pi r^2 g_{\alpha\beta}(r)dr, \tag{1}$$

where ρ_β is the number density of β-type atoms, and $R_{\alpha\beta}$ is a cutoff distance determined from the first-minimum position of $g_{\alpha\beta}(r)$. Table I shows the Cu-concentration dependence of $N_{\alpha\beta}$. If there were no wrong As-As and S-S bonds in the case of x=0.0, N_{AsS} and N_{SAs} would be three and two, respectively, and both N_{AsAs} and N_{SS} would be zero. It is, however, seen that N_{AsS} and N_{SAs} are smaller than their respective ideal values, and that N_{AsAs} and N_{SS} have finite values. Note that $N_{\mathrm{AsS}}+N_{\mathrm{AsAs}}$ and $N_{\mathrm{SAs}}+N_{\mathrm{SS}}$ are almost three and two, respectively, i.e., As and S atoms have threefold and twofold coordinations, respectively, with some homopolar bonds at x=0.0. With increasing Cu concentration x, N_{AsAs} increases, while N_{AsS} (N_{SAs}) decreases. This is consistent with the fact that N_{CuS} has larger values (~3) than N_{CuAs} ($\leq$0.56), implying that Cu atoms prefer to bind with S atoms as described

TABLE I. Coordination number $N_{\alpha\beta}$ of amorphous $Cu_x(As_{0.4}S_{0.6})_{1-x}$. The cutoff distances $R_{\alpha\beta}$ used in the calculation of $N_{\alpha\beta}$ are also shown.

	$N_{\alpha\beta}$			
	x=0.0	x=0.024	x=0.11	$R_{\alpha\beta}$ (Å)
As-As	0.25	0.31	0.55	2.8
As-S	2.79	2.69	2.38	2.7
As-Cu		0.01	0.18	2.8
S-As	1.86	1.79	1.59	2.7
S-S	0.17	0.17	0.17	2.5
S-Cu		0.13	0.61	2.7
Cu-As		0.09	0.56	2.8
Cu-S		3.10	2.95	2.7
Cu-Cu			0.35	2.9

above. Most Cu atoms added will occupy positions near S atoms by taking the place of As atoms, and As atoms excluded from the vicinity of S atoms will bind to each other. The calculated coordination number of Cu atoms reaches about 3.9 ($=N_{CuAs}+N_{CuS}+N_{CuCu}$) in total at $x=0.11$, which is in accord with the prediction of a formal-valence-shell model.[37] It is interesting to note that the Cu-concentration dependence of $g_{\alpha\beta}(r)$ and $N_{\alpha\beta}$ for As-As, S-S, and As-S pairs resembles the temperature dependence of these quantities observed in liquid As_2S_3.[38] In the liquid state, the bond breaking and bond exchange in the network structure are induced by thermal motion of atoms at higher temperatures.

C. Details of atomic coordinations

To investigate the atomic coordination around each atom in more detail, we define two quantities, $P_\alpha^{\rm all}(n)$ and $P_\alpha^{\rm host}(n)$, called the coordination-number distribution functions. Both quantities are the ratio of the number of α-type atoms with coordination number n to the total number of α-type atoms. First, we counted the number of β-type atoms, $n_\beta(i)$, inside a sphere with a radius $R_{\alpha\beta}$ centered at the ith atom ($i\in\alpha$). We used the same values of $R_{\alpha\beta}$ as those in the calculation of $N_{\alpha\beta}$. Then, $P_\alpha^{\rm all}(n)$ and $P_\alpha^{\rm host}(n)$ were obtained from distributions of $n^{\rm all}(i)=n_{\rm As}(i)+n_{\rm S}(i)+n_{\rm Cu}(i)$ and $n^{\rm host}(i)=n_{\rm As}(i)+n_{\rm S}(i)$, respectively, for $i\in\alpha$. Note that they were calculated by taking the time average, and were normalized as $\Sigma_n P_\alpha^{\rm all}(n)=1$ and $\Sigma_n P_\alpha^{\rm host}(n)=1$. Figure 5 displays $P_\alpha^{\rm all}(n)$ and $P_\alpha^{\rm host}(n)$ for $x=0.0$, 0.024, and 0.11. It is seen from $P_{\rm As}^{\rm all}(n)$ that more than 90% of As atoms have threefold coordination at all x, and fourfold coordinated As atoms increases slightly with increasing x. At $x=0.11$, the ratio of the number of As atoms coordinated with two host (As or S) atoms [$P_{\rm As}^{\rm host}(2)$] is about 0.1. When the number of atoms coordinated with the As atoms is counted by including Cu atoms, almost no As atoms have twofold coordination, as $P_{\rm As}^{\rm all}(2)$ is nearly zero. This means that there are one or two Cu atoms neighboring to the As atoms that are coordinated with two host atoms. The Cu concentration dependence of

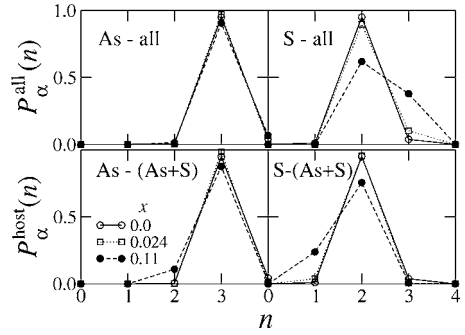

FIG. 5. Coordination-number distribution functions $P_\alpha^{\rm all}(n)$ and $P_\alpha^{\rm host}(n)$ of amorphous $Cu_x(As_{0.4}S_{0.6})_{1-x}$. The open circles, open squares, and solid circles show $P_\alpha^{\rm all}(n)$ and $P_\alpha^{\rm host}(n)$ for $x=0.0$, 0.024, and 0.11, respectively.

$P_{\rm S}^{\rm all}(n)$ reveals that the coordination-number distribution around S atoms at $x=0.11$ is markedly different from those at $x=0.0$ and 0.024. About 60% of S atoms have twofold coordination, and the rest have threefold coordination at $x=0.11$. There is a noticeable difference between $P_{\rm S}^{\rm all}(n)$ and $P_{\rm S}^{\rm host}(n)$ at $x=0.11$, reflecting the distribution of Cu atoms around S atoms. These results are in accord with the previous suggestion[37] based on x-ray diffraction experiments that the addition of Cu atoms reduces the fraction of S atoms that are twofold coordinated. It should be noted that both $P_{\rm As}^{\rm host}(4)$ and $P_{\rm S}^{\rm host}(3)$ have finite values at $x=0.0$, and they become nearly zero when Cu atoms are added. This means that Cu atoms suppress the overcoordination between host atoms.

In a similar way to $P_\alpha^{\rm all}(n)$ and $P_\alpha^{\rm host}(n)$, we obtained partial quantities $P_{\alpha\beta}(n)$ from the distribution of $n_\beta(i)$ for $i\in\alpha$ as shown in Fig. 6. For all x, $P_{\rm AsAs}(n)$ and $P_{\rm SS}(n)$ have the largest values at $n=0$, and decrease monotonically as n increases. While $P_{\rm SS}(n)$ has only a weak dependence on x,

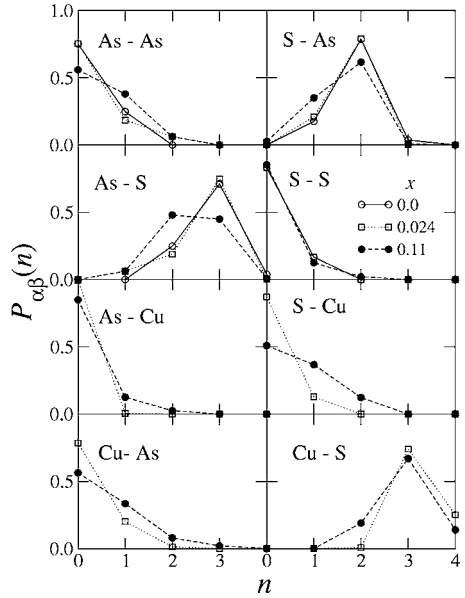

FIG. 6. Coordination-number distribution functions $P_{\alpha\beta}(n)$ of amorphous $Cu_x(As_{0.4}S_{0.6})_{1-x}$. The open circles, open squares, and solid circles show $P_{\alpha\beta}(n)$ for $x=0.0$, 0.024, and 0.11, respectively.

$P_{AsAs}(n)$ depends somewhat on x, i.e., $P_{AsAs}(1)$ and $P_{AsAs}(2)$ increase with increasing x, and $P_{AsAs}(0)$ decreases. More remarkable effects of the addition of Cu atoms are found in $P_{AsS}(n)$ and $P_{SAs}(n)$. When the Cu concentration is low (x=0.0 and 0.024), almost 75% of As atoms have three S atoms as their neighbors, and more than 80% of S atoms have two neighboring As atoms. At x=0.11, the ratio of these atoms decreases, and those atoms which have lower coordinations increase, especially $P_{AsS}(2)$ has a comparable value to $P_{AsS}(3)$.

As seen from $P_{AsCu}(n)$, there are few Cu atoms coordinated with As atoms at x=0.024, and about 15% of As atoms have one neighboring Cu atom at x=0.11. On the other hand, there exist more Cu atoms around S atoms, i.e., at x=0.11, the ratios of onefold and twofold Cu-coordinated S atoms reach 35% and 15%, respectively, although $P_{SCu}(0)$ has the largest value (~50%). Around Cu atoms, more S atoms exist than As atoms. At both x=0.024 and 0.11, there exist three S atoms around Cu atoms in most cases as $P_{CuS}(n)$ has a high peak at n=3. In contrast, only one or two As atoms exist around Cu atoms even at x=0.11. We have observed that some Cu atoms change their coordinations with time, although they do not show any diffusive motion, i.e., they move locally between sites that have almost the same local energy minima. The residence time at each site is of the order of 0.1–1 ps. On the other hand, the coordinations between host atoms change very occasionally around the coordination defects at all x.

Up to here, we examine the coordination-number distribution based on pairs of atomic species. To clarify the characteristics of structural change by the addition of Cu atoms, it is valuable to investigate the distribution of atomic coordinations by classifying atoms by three numbers (n_{As},n_S,n_{Cu}), where n_{As},n_S,n_{Cu} are the number of neighboring As, S, and Cu atoms, respectively, to the atoms considered. We obtained the ratio $p_\alpha(n_{As},n_S,n_{Cu})$ of the number of α-type atoms, which are coordinated with n_{As} As atoms, n_S S atoms, and n_{Cu} Cu atoms, to the total number of α-type atoms. As was seen in Fig. 5, more than 90% of As atoms have threefold coordination. From $p_{As}(n_{As},n_S,n_{Cu})$ for As atoms shown in Fig. 7, we can see the details of the distribution. At x=0.0, about 70% of As atoms have (0,3,0) coordination, i.e., they neighbor to three S and no As atoms. About 25% of As atoms have (1,2,0) coordination, and about 4% have (0,4,0) overcoordination. At x=0.024, the (0,3,0)-coordinated As atoms increase slightly, and instead the (0,4,0)-coordinated and (1,2,0)-coordinated As atoms decrease. This implies that, when the Cu concentration is low, Cu atoms prefer to stay in such environments that the stoichiometric atomic concentration corresponding to x=0.0 is disrupted locally. Note that there appear the (2,1,0)-coordinated As atoms (about 6%), which results from the assembly of As atoms excluded from the positions near S atoms by Cu atoms. When x reaches 0.11, the number of (0,3,0)-coordinated As atoms is reduced largely, and the (1,2,0)-coordinated As atoms increase. Cu atoms neighbor to As atoms as well as to S atoms at this Cu concentration, and some As atoms have (0,2,1), (1,2,1), (0,3,1), and (0,2,2) coordinations. It is emphasized that the (0,2,1)-coordinated, (0,2,2)-coordinated, and (0,2,0)-coordinated As atoms, which are undercoordinated with host atoms, appear or increase. Around these atoms, there are large amplitudes of the electronic wave functions of unoccupied states near the bottom of the conduction band, which are not seen in the amorphous states at x=0.0. The related discussions to this point will be made in Sec. IV.

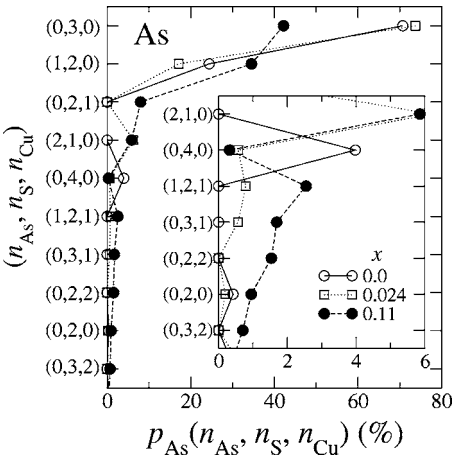

FIG. 7. Ratio $p_{As}(n_{As},n_S,n_{Cu})$ of the number of the (n_{As},n_S,n_{Cu})-coordinated As atoms to the total number of As atoms. The open circles, open squares, and solid circles show $p_{As}(n_{As},n_S,n_{Cu})$ for x=0.0, 0.024, and 0.11, respectively. In the inset, the scale of the horizontal axis is magnified.

Figure 8 shows $p_S(n_{As},n_S,n_{Cu})$ for S atoms. At x=0.0, there are a few overcoordinated-(3,0,0) and undercoordinated-(1,0,0) S atoms, besides many twofold (2,0,0)-coordinated and (1,1,0)-coordinated S atoms. Similar to the coordination around As atoms, the nonstoichiometric (3,0,0)-coordinated and (1,0,0)-coordinated S atoms almost disappear when Cu atoms are added. At x=0.024, the number of (2,0,0)-coordinated S atoms are reduced, and instead the (2,0,1)-coordinated and (1,0,1)-coordinated S atoms appear. With the increase of x to 0.11, the (2,0,1)-coordinated,

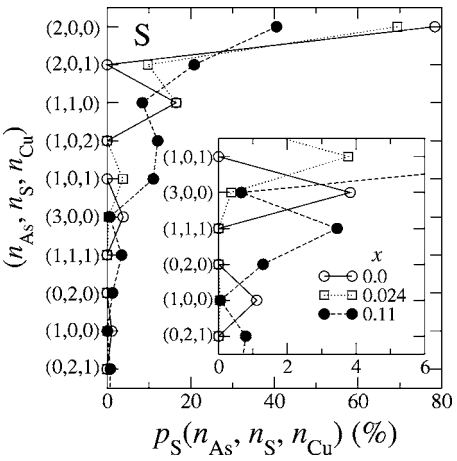

FIG. 8. Ratio $p_S(n_{As},n_S,n_{Cu})$ of the number of the (n_{As},n_S,n_{Cu})-coordinated S atoms to the total number of S atoms. The open circles, open squares, and solid circles show $p_S(n_{As},n_S,n_{Cu})$ for x=0.0, 0.024, and 0.11, respectively. In the inset, the scale of the horizontal axis is magnified.

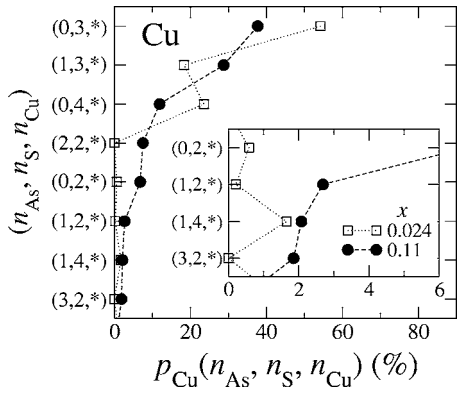

FIG. 9. Ratio $p_{Cu}(n_{As},n_S,n_{Cu})$ of the number of the (n_{As},n_S,n_{Cu})-coordinated Cu atoms to the total number of Cu atoms. In the figure, ratios summed with respect to n_{Cu} are plotted. The open squares and solid circles show $p_{Cu}(n_{As},n_S,n_{Cu})$ for $x=0.024$ and 0.11, respectively. In the inset, the scale of the horizontal axis is magnified.

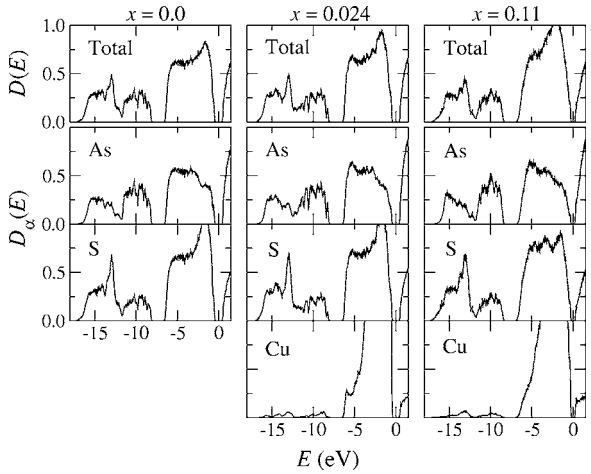

FIG. 10. Total $D(E)$ and partial $D_\alpha(E)$ electronic densities of states of amorphous $Cu_x(As_{0.4}S_{0.6})_{1-x}$. The origin of the energy is taken to be the Fermi level ($E_F=0$).

(1,0,2)-coordinated, (1,0,1)-coordinated, and (1,1,1)-coordinated S atoms increase largely, reflecting the fact that the favorable sites to Cu atoms are around S atoms, accompanied with the reductions of the (2,0,0)-coordinated and (1,1,0)-coordinated S atoms.

Figure 9 displays $p_{Cu}(n_{As},n_S,n_{Cu})$ for Cu atoms. In the figure, ratios summed with respect to n_{Cu} are plotted to avoid complexity, and the coordinations are expressed as $(n_{As},n_S,*)$. As was seen in Fig. 6, about 70% of Cu atoms neighbor to three S atoms at $x=0.024$. We see from the ratio of $(1,3,*)$-coordinated Cu atoms $[p_{Cu}(1,3,*)$ in Fig. 9] that about 20% of Cu atoms neighbor to one As atoms as well as three S atoms. While the $(0,3,*)$-coordinated and $(0,4,*)$-coordinated Cu atoms decrease when x reaches 0.11, the Cu atoms with coordinations of $(1,3,*)$, $(2,2,*)$, $(1,2,*)$, and so on, which neighbor to As atoms, increase. As stated above, Cu atoms change their sites locally with time. We have observed that there occur the coordination changes of $(0,3,*)\leftrightarrow(1,3,*)$ and $(0,3,*)\leftrightarrow(0,4,*)$ at both $x=0.024$ and 0.11. Furthermore, the coordination changes of $(0,3,*)\leftrightarrow(0,2,*)$ and $(3,2,^*)\leftrightarrow(2,2,*)$ take place at $x=0.11$. Such local backward and forward motions of metal atoms will be important for dynamic processes in metal-doped amorphous chalcogenides.

D. Electronic density of states

Figure 10 shows the total electronic density of states (DOS), $D(E)$, and the partial DOS, $D_\alpha(E)$, for α-type atoms for $x=0.0$, 0.024, and 0.11. We calculated $D_\alpha(E)$ from the weights of the electronic states to each atom, obtained by expanding the electronic wavefunctions in atomic orbitals. [39] For all x, the electronic states between −17 and −8 eV consist of the 4s states of As atoms and the 3s states of S atoms. At $x=0.0$, the electronic states above −6 eV are formed by the 4p states of As atoms and the 3p states of S atoms; the p-like states below the Fermi level (E_F) are the σ-type bonding states between neighboring atoms, and those above E_F are the σ^*-type antibonding states. Also, the peak at about −2 eV in $D_S(E)$ corresponds to the lone-pair states around S atoms. By the addition of Cu atoms, the total $D(E)$ is altered appreciably in the energy range between −3 and 0 eV. In particular, $D_S(E)$ changes largely, i.e., the peaked shape of $D_S(E)$ present in the valence band top at $x=0.0$ is reduced with increasing x. It is seen from $D_{Cu}(E)$ that the 3d states of Cu atoms spread over the same energy range as the p states of As and S atoms, which indicates that mixed electronic states are formed by these states, especially by the copper 3d and sulfur lone-pair states.

The total DOS $D(E)$ and the partial DOS $D_\alpha(E)$ near E_F in the energy range between −1 and 1 eV are displayed in Fig. 11. It is found that the energy gap in $D(E)$ at E_F is

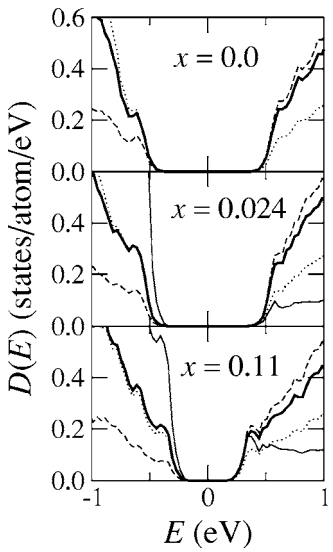

FIG. 11. Total $D(E)$ and partial $D_\alpha(E)$ electronic densities of states of amorphous $Cu_x(As_{0.4}S_{0.6})_{1-x}$. The bold solid lines show the total $D(E)$. The dashed, dotted, and thin solid lines show the partial $D_\alpha(E)$ for α=As, S, and Cu atoms, respectively. The origin of the energy is taken to be the Fermi level ($E_F=0$).

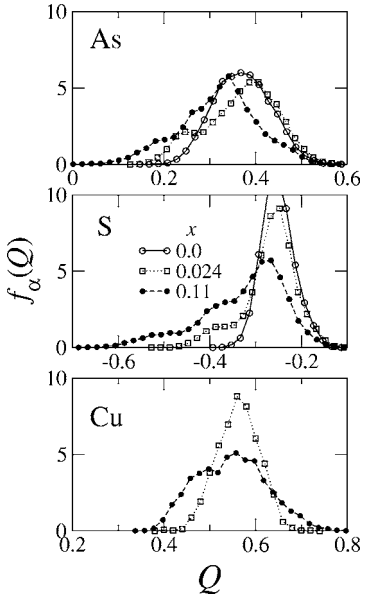

FIG. 12. Distributions $f_\alpha(Q)$ of the gross charges $Q_{i\in\alpha}$. The open circles, open squares, and solid circles show $f_\alpha(Q)$ for $x=0.0$, 0.024, and 0.11, respectively.

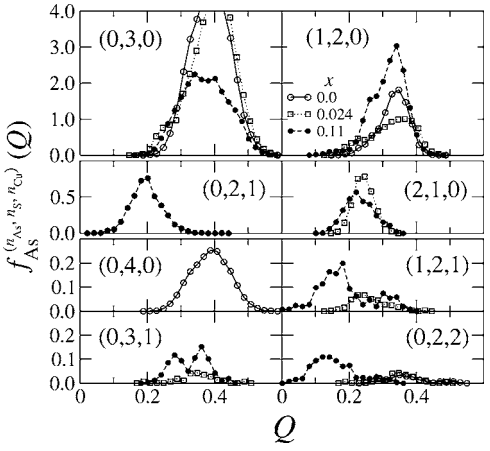

FIG. 13. Distributions $f_{\mathrm{As}}^{(n_{\mathrm{As}},n_{\mathrm{S}},n_{\mathrm{Cu}})}(Q)$ of the gross charges $Q_{i\in\mathrm{As}}$ for the $(n_{\mathrm{As}},n_{\mathrm{S}},n_{\mathrm{Cu}})$-coordinated As atoms. The open circles, open squares, and solid circles show $f_{\mathrm{As}}^{(n_{\mathrm{As}},n_{\mathrm{S}},n_{\mathrm{Cu}})}(Q)$ for $x=0.0$, 0.024, and 0.11, respectively.

reduced with increasing x. Although the approximation to the exchange correlation in the density-functional theory usually gives the energy gap smaller than the exact value, the trend is similar to the behavior observed experimentally for Ag-doped and Cu-doped As_2Se_3.[40] Near the top of the valence band, $D_{\mathrm{Cu}}(E)$ and $D_{\mathrm{As}}(E)$ have the largest and smallest values, respectively, while they are reversed near the bottom of the conduction band. It should be emphasized that the contribution of $D_{\mathrm{Cu}}(E)$ near the bottom of the conduction band becomes more important with increasing x. The related discussions are given below.

E. Mulliken charges

To investigate charges on each atom and bonding properties between atoms, we used the population analysis[41,42] by expanding the electronic wave functions in atomic-orbital basis sets.[43,44] Based on the formulation for the ultrasoft pseudopotentials,[39] we calculated the gross charge[41] Q_i for the ith atom, which measures the ionicity of each atom. We also obtained the overlap population[41] O_{ij} between the i th and jth atoms as discussed in the next subsection, which gives a semiquantitative estimate of the strength of covalent-like bonding between atoms.[44] It should be noted that, since the atomic-orbital basis used in the expansion of the wave functions is not unique, the absolute magnitudes of Q_i and O_{ij} have little physical meaning.[44] A different set of atomic-orbital bases would give different values for these quantities. However, we can discuss their relative magnitudes meaningfully, because the trends are the same for any choice of atomic-orbital basis sets. For the basis used in our calculations, the charge spillage[43] defining the error in the expansion is less than 0.3%.

Figure 12 shows the distribution, $f_\alpha(Q)$, of $Q_{i\in\alpha}$ for α-type atoms. Note that $f_\alpha(Q)$ is normalized as $\int f_\alpha(Q)\mathrm{d}Q=1$. When there is no Cu atom in the system ($x=0.0$), both $f_{\mathrm{As}}(Q)$ and $f_{\mathrm{S}}(Q)$ have nearly symmetric shapes, which have peaks at about $Q=0.37$ and -0.27, respectively. At $x=0.024$, there appear shoulders in $f_{\mathrm{As}}(Q)$ and $f_{\mathrm{S}}(Q)$ at about $Q=0.25$ and -0.37, respectively, due to the transferred electrons from Cu atoms to host atoms. $f_{\mathrm{Cu}}(Q)$ has a peak at about $Q=0.56$. If more Cu atoms are added and x approaches 0.11, more electrons transfer from Cu atoms to As and S atoms, and as a result the shapes of $f_{\mathrm{As}}(Q)$ and $f_{\mathrm{S}}(Q)$ become very asymmetric with peaks at about $Q=0.34$ and -0.28, respectively. The atomic charges of Cu atoms have a wide distribution with tails on both larger and smaller Q sides as displayed by $f_{\mathrm{Cu}}(Q)$.

To analyze the Cu-concentration dependence of $f_\alpha(Q)$ in detail, we decomposed $f_\alpha(Q)$ into $f_\alpha^{(n_{\mathrm{As}},n_{\mathrm{S}},n_{\mathrm{Cu}})}(Q)$ with the atomic coordinations $(n_{\mathrm{As}},n_{\mathrm{S}},n_{\mathrm{Cu}})$ of α-type atoms. Note that the sum of $f_\alpha^{(n_{\mathrm{As}},n_{\mathrm{S}},n_{\mathrm{Cu}})}(Q)$ with respect to the coordinations gives $f_\alpha(Q)$. Figures 13–15 show $f_\alpha^{(n_{\mathrm{As}},n_{\mathrm{S}},n_{\mathrm{Cu}})}(Q)$ for $\alpha=$As, S, and Cu, respectively. It is seen that the distribution ranges shown by $f_\alpha^{(n_{\mathrm{As}},n_{\mathrm{S}},n_{\mathrm{Cu}})}(Q)$ depend on the atomic coordinations $(n_{\mathrm{As}},n_{\mathrm{S}},n_{\mathrm{Cu}})$, which reflects the fact that the atomic charges are determined by the local configuration of atoms.

For the As atoms with (0,3,0) coordination, the atomic charges are distributed over $Q=0.2-0.5$ with a peak at about $Q=0.4$ at all x [$f_{\mathrm{As}}^{(0,3,0)}(Q)$ in Fig. 13]. If one of the three neighboring S atom is replaced by an As atom, the distribution in larger Q region is reduced, and the atomic charges are distributed over $Q=0.2-0.4$ [$f_{\mathrm{As}}^{(1,2,0)}(Q)$ in Fig. 13]. For the As atoms with (2,1,0) coordination, which are not found at $x=0.0$, the atomic charges are distributed over $Q=0.15-0.3$ [$f_{\mathrm{As}}^{(2,1,0)}(Q)$ in Fig. 13], which gives the shoulder in $f_{\mathrm{As}}(Q)$ at about $Q=0.25$ (at $x=0.024$). For the As atoms that neighbor to Cu atoms at $x=0.11$, the distributions of the atomic charges have peaks at smaller values of $Q<0.2$ [$f_{\mathrm{As}}^{(0,2,1)}(Q)$, $f_{\mathrm{As}}^{(1,2,1)}(Q)$, and $f_{\mathrm{As}}^{(0,2,2)}(Q)$ in Fig. 13]. The asymmetric shape of $f_{\mathrm{As}}(Q)$ comes from the atomic charges of those As atoms.

The Cu-concentration dependence of $f_{\mathrm{S}}(Q)$ (Fig. 12) is explained by $f_{\mathrm{S}}^{(n_{\mathrm{As}},n_{\mathrm{S}},n_{\mathrm{Cu}})}(Q)$ shown in Fig. 14; (1) the main

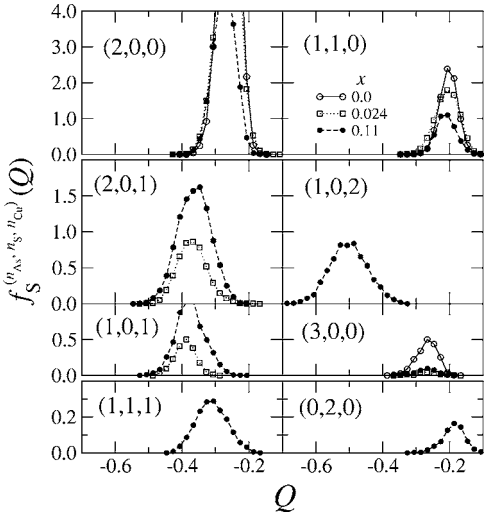

FIG. 14. Distributions $f_{\mathrm{S}}^{(n_{\mathrm{As}},n_{\mathrm{S}},n_{\mathrm{Cu}})}(Q)$ of the gross charges $Q_{i\in\mathrm{S}}$ for the $(n_{\mathrm{As}},n_{\mathrm{S}},n_{\mathrm{Cu}})$-coordinated S atoms. The open circles, open squares, and solid circles show $f_{\mathrm{S}}^{(n_{\mathrm{As}},n_{\mathrm{S}},n_{\mathrm{Cu}})}(Q)$ for $x=0.0$, 0.024, and 0.11, respectively.

peak of $f_{\mathrm{S}}(Q)$ comes from the distribution of the atomic charges of S atoms that neighbor to no Cu atom, mainly the (2,0,0)-coordinated S atoms, (2) the shoulder at about $Q=-0.37$ (at $x=0.024$) is contributed by the (2,0,1)-coordinated and (1,0,1)-coordinated S atoms, and (3) the asymmetric shape at $x=0.11$ results from the appearance of the (1,0,2)-coordinated S atoms, as well as the increase of the (2,0,1)-coordinated and (1,0,1)-coordinated S atoms.

It is obvious from Fig. 15 that the main contribution to $f_{\mathrm{Cu}}(Q)$ at $x=0.024$ is made by the distribution of the atomic charges of $(0,3,*)$-coordinated Cu atoms. At $x=0.11$, the $(1,3,*)$-coordinated Cu atoms increase as was seen in Fig. 9, and the atomic charges of those atoms spread over a wider Q range. The atomic charges of $(0,4,*)$-coordinated, $(2,2,*)$-coordinated, and $(0,2,*)$-coordinated Cu atoms are distributed over rather narrow Q ranges, and their peak positions depend on coordinations.

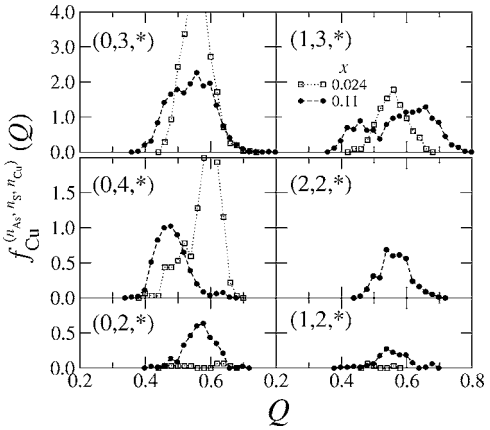

FIG. 15. Distributions $f_{\mathrm{Cu}}^{(n_{\mathrm{As}},n_{\mathrm{S}},n_{\mathrm{Cu}})}(Q)$ of the gross charges $Q_{i\in\mathrm{Cu}}$ for the $(n_{\mathrm{As}},n_{\mathrm{S}},n_{\mathrm{Cu}})$-coordinated Cu atoms. In the figure, values summed with respect to n_{Cu} are plotted. The open squares and solid circles show $f_{\mathrm{Cu}}^{(n_{\mathrm{As}},n_{\mathrm{S}},n_{\mathrm{Cu}})}(Q)$ for $x=0.024$ and 0.11, respectively.

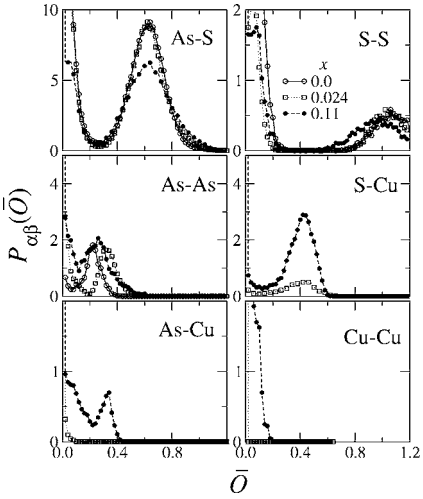

FIG. 16. Distributions $P_{\alpha\beta}(\bar{O})$ of the overlap populations $O_{i\in\alpha,j\in\beta}$ for six pairs of α-atomic and β-atomic types. The open circles, open squares, and solid circles show $P_{\alpha\beta}(\bar{O})$ for $x=0.0$, 0.024, and 0.11, respectively.

F. Bond-overlap populations

Figure 16 shows time averaged distributions $P_{\alpha\beta}(\bar{O})$ of the bond-overlap populations $O_{i\in\alpha,j\in\beta}$ for six pairs of α-atomic and β-atomic types. Note that the integration of $P_{\alpha\beta}(\bar{O})$, $\int_{O_{\min}}^{\infty}P_{\alpha\beta}(\bar{O})\mathrm{d}\bar{O}$, gives the average number of β-type atoms, which have the bond-overlap populations greater than $O_{\min}$ with α-type atoms, around one α-type atom.

For pairs of As and S atoms, $P_{\mathrm{AsS}}(\bar{O})$ has a clear peak at about $\bar{O}=0.5$ regardless of x. The peak height becomes lower with increasing x reflecting the decrease of the number of As-S atomic pairs. The homopolar S-S atomic pairs have larger bond-overlap populations over the range of $\bar{O}=0.8-1.3$ than those between the As-S pairs, which means that the covalent bonds between neighboring S atoms are stronger than those between As and S atoms in spite of energetically unfavorable pairs. For As-As pairs, the bond-overlap populations are distributed over $\bar{O}<0.45$ with a peak at about $\bar{O}\sim0.2$, which is smaller than those for the As-S and S-S pairs. In $P_{\mathrm{SCu}}(\bar{O})$ and $P_{\mathrm{AsCu}}(\bar{O})$, there are also peaks at about $\bar{O}=0.4$ and 0.35, respectively, which clearly shows that Cu atoms interact with neighboring S and As atoms by a covalentlike bonding. The fact that $P_{\mathrm{CuCu}}(\bar{O})$ spreads over $\bar{O}\sim0.2$ at $x=0.11$ although no peak is found, implies that there is a weak covalentlike interaction between Cu atoms, which gives the peak in $g_{\mathrm{CuCu}}(r)$ at about $r=2.8$ Å (Fig. 4).

IV. DISCUSSION

The structural results shown in Figs. 4 and 6 have revealed that Cu atoms have a short-range correlation with S atoms similar to that between As and S atoms. As was shown by the bond-overlap populations, there is a formation of covalentlike bonds between Cu and S atoms, which gives the

short-range correlation. On the other hand, we have observed that the As-S first coordination shell is clearly seen in $g_{AsS}(r)$ (Fig. 3) in spite of the formation of a large number of Cu-S bonds. Also, more than half of S atoms that neighbor to Cu atoms bind to two host (As and S) atoms, as shown in Fig. 8. These results lead to the conclusion that most of the σ-type bonding states remain around S atoms besides the formations of the Cu-S bonds, and that large portions of Cu-S bonds are formed by using the $3p$ electrons of S atoms, which were in the lone-pair orbitals in As_2S_3, and the $3d$ electrons of Cu atoms. Since the energy range corresponding to the lone-pair states spreads due to the bond formation, there occurs the reduction of the peaked shape in $D_S(E)$ as displayed in Fig. 10. It is noted that N_{SAs} (the number of As atoms coordinated with a S atom) decreases from 1.9 to 1.6 by doping with Cu atoms (Table I), and that there exist some S atoms which bind to only one As atom in addition to Cu atoms especially at $x=0.11$ (Fig. 8). Since these S atoms undercoordinated with As atoms have more electrons than the twofold coordinated S atoms as was shown by the distribution of the gross charges (Fig. 14), the dangling bonds of the undercoordinated S atoms are probably stabilized by the transferred electrons from Cu atoms.

Next, we discuss the atomic structure and electronic states in Cu-doped arsenic chalcogenides in connection with photoinduced phenomena. Simdyankin *et al.*[21] have found from their tight-binding calculations that there exist defect pairs, $[As_4]^-$-$[S_3]^+$, in amorphous As_2S_3. They have suggested that the conversion from the ordinary coordination defects into the $[As_4]^-$-$[S_3]^+$ defect pairs under illumination could contribute to photodarkening. They have also studied the influence of alloying Cu atoms,[22] and have asserted that the sulfur lone-pair states are pushed down in energy by the addition of Cu atoms, and that the additional Cu states with the same energies as the states due to the $[As_4]^-$-$[S_3]^+$ defect pairs are responsible for masking photodarkening. Our *ab initio* results described in Sec. III are compatible with their suggestions. As shown in Figs. 7 and 8 there exist a few coordination defects such as the (0,4,0)-coordinated As and (3,0,0)-coordinated and (1,0,0)-coordinated S atoms in Cu-free amorphous As_2S_3. These defects would be easily converted to other types of defects such as the $[As_4]^-$-$[S_3]^+$ defect pair under illumination, which would give rise to photodarkening according to the suggestion of Simdyankin *et al.* We have observed that the coordination defects in pure As_2S_3 decrease by the addition of Cu atoms. This reduction of the coordination defects will suppress the generation of the $[As_4]^-$-$[S_3]^+$ defect pairs in Cu-doped As_2S_3 under illumination, which means the suppression of photodarkening. The reduction of the peaked shape of the lone-pair states in $D_S(E)$ by doping with Cu atoms is also consistent with the observation of Simdyankin *et al.*

From Fig. 11, we have seen that the partial DOS for Cu atoms increases near the bottom of the conduction band with increasing the Cu concentration, accompanied with the reduction of the energy gap in the total DOS at the Fermi level. At $x=0.11$, $D_{Cu}(E)$ is comparable in value to $D_{As}(E)$ around the energy of $E=0.4$ eV. To clarify the electronic states near the Fermi level in Cu-doped As_2S_3, the spatial distribution of

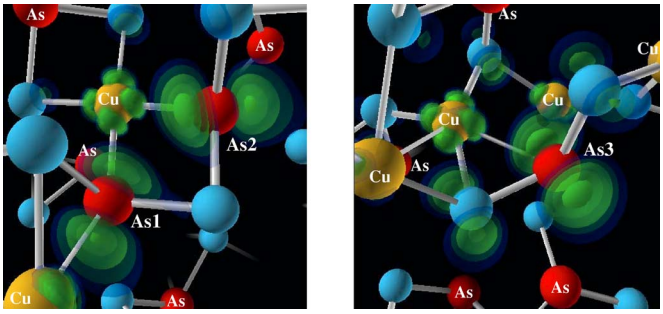

FIG. 17. (Color online) Spatial distributions of the electronic wave functions of two states near the bottom of the conduction band at $x=0.11$. The positions of As and Cu atoms are shown by the balls with "As" (red) and "Cu" (yellow), respectively. The (blue) balls without symbols show the positions of S atoms. The bonds connect two atoms with atomic distances being less than $R_{\alpha\beta}$ listed in Table I.

electronic wave functions was investigated. We have confirmed that near the top of the valence band the $3p$ lone-pair states of S atoms are mixed with the $3d$ states of Cu atoms as suggested by Simdyankin *et al.*[22] The spatial distribution of the wave functions for the states near the bottom of the conduction band, more precisely, for the first and the second states counting from the bottom of the conduction band, is shown in Fig. 17. We see from this figure that (1) the states near the bottom of the conduction band are localized around a few atoms, mainly As and Cu atoms, (2) those states are mostly formed by the $3d$ states of Cu atoms and the $4p$ states of As atoms, and (3) around As and S atoms, those states have the spatial distribution of the lone-pair states. We notice that the wave functions have large amplitudes around the As atoms labeled As1, As2, and As3. The coordination numbers (n_{As}, n_S, n_{Cu}) are (0,2,2), (0,2,1), and (0,2,0) for As1, As2, and As3, respectively, where n_{As}, n_S, n_{Cu} are the number of neighboring As, S, and Cu atoms, respectively. Note that the number of neighboring S atoms to these three As atoms is two. As displayed in Fig. 7, such (0,2,1)-coordinated, (0,2,2)-coordinated, and (0,2,0)-coordinated As atoms increase with increasing the Cu concentration, whereas the overcoordinated (0,4,0)-As atoms decrease.

Around the As atoms coordinated with two chalcogen atoms, the same electronic states associated with the p electrons will take place as those around the two-fold coordinated chalcogen atoms, i.e., the twofold coordinated bonding states and the lone-pair states. To occupy these states, four p electrons per atom are needed, as is the case for chalcogen atoms. However, since the number of $4p$ electrons of As atom is three, the lone-pair states around the twofold coordinated As atoms will not be occupied completely. Some of such lone-pair states form the unoccupied states mixed with the $3d$ states of Cu atoms near the bottom of the conduction band as shown in Fig. 17. Since those states have nonbonding character, significant structural changes will not take place by the excitation of electrons, and the photodarkening will be suppressed under illumination. We conclude that the appearance of the As atoms coordinated with two chalcogen atoms such as the (0,2,1)-coordinated, (0,2,2)-coordinated, and (0,2,0)-coordinated As atoms could be one of the mecha-

nisms of the suppression of photodarkening in Cu-doped arsenic chalcogenides.

V. SUMMARY

The atomic structure and bonding properties in amorphous Cu_x (As_2S_3) (x=0, 0.024, and 0.11) have been studied by *ab initio* MD simulations. It is shown from the partial radial distribution functions and the coordination numbers that Cu atoms prefer to bind with S atoms. The number of As atoms coordinated with As atoms increases with increasing Cu concentration, while the number of S atoms coordinated with S atoms remains unchanged. From the detailed studies of the coordination-number distribution functions, we have seen that Cu atoms suppress the overcoordination between host (As and S) atoms. We have also seen that As atoms undercoordinated with two S atoms increase by the addition of Cu atoms. Around these As atoms, there are large amplitudes of the electronic wave functions of the unoccupied states near the bottom of the conduction band, which will play an important role in the suppression of photodarkening in Cu-doped arsenic chalcogenides. It is shown from the electronic DOS that, with increasing the Cu concentration, the peaked shape of the partial DOS for S atoms near the valence band top is reduced due to the mixing of the lone-pair 3p states of S atoms with the 3d states of Cu atoms, and the contributions of the partial DOS for Cu atoms as well as that for As atoms become important near the bottom of the conduction band accompanied with the reduction of the band gap at the Fermi level. We have examined the bonding properties of atoms by the population analysis. It is found from Mulliken charges that the ionicity of S atoms is enhanced, while that of As atoms decreases due to the electron transfer from Cu atoms, and that the charge of each atom depends on the atomic coordination. The examination of bond-overlap populations shows that Cu atoms interact with neighboring S and As atoms by a covalentlike bonding.

ACKNOWLEDGMENTS

The present work was supported in part by the Grant-in-Aid for Scientific Research on Priority Area, "Materials Science of Metallic Glasses (428)" and "Nanoionics (439)," and the Grant-in-Aid for Scientific Research (C) by the Ministry of Education, Culture, Sports, Science and Technology of Japan. The authors thank the Supercomputer Center, Institute for Solid State Physics, University of Tokyo for the use of the facilities.

[1] Y. Iwadate, T. Hattori, S. Nishiyama, K. Fukushima, Y. Mochizuki, M. Misawa, and T. Fukunaga, J. Phys. Chem. Solids **60**, 1447 (1999).
[2] M. A. Popescu, *Non-Crystalline Chalcogenides* (Kluwer Academic, Dordrecht, 2000).
[3] A. E. Owen, A. P. Firth, and P. J. S. Ewen, Philos. Mag. B **52**, 347 (1985).
[4] K. Tanaka, Rev. Solid State Sci. **4**, 641 (1990).
[5] G. Pfeiffer, M. A. Paesler, and S. C. Agarwal, J. Non-Cryst. Solids **130**, 111 (1991).
[6] K. Shimakawa, A. Kolobov, and S. R. Elliott, Adv. Phys. **44**, 475 (1995).
[7] M. Frumar, Z. Polák, Z. Černošek, B. Frumarová, and T. Wágner, Chem. Papers **51**, 310 (1997).
[8] K. Tanaka, Phys. Rev. B **57**, 5163 (1998).
[9] I. Z. Indutnyi and P. E. Shepeljavi, J. Non-Cryst. Solids **227-230**, 700 (1998).
[10] P. Hari, S. Guzel, T. Su, P. C. Taylor, P. L. Kuhns, W. G. Moulton, and N. S. Sullivan, J. Non-Cryst. Solids **326-327**, 199 (2003).
[11] K. Tanaka, Appl. Phys. Lett. **26**, 243 (1975).
[12] J. Z. Liu and P. C. Taylor, Phys. Rev. Lett. **59**, 1938 (1987).
[13] A. Matsuda, M. Kumeda, and T. Shimizu, Jpn. J. Appl. Phys., Part 2 **30**, L1075 (1991).
[14] G. B. Turpin and L. E. McNeil, Phys. Rev. B **39**, 8750 (1989).
[15] A. Gheorghiu-de La Rocque, E. Belin-Ferré, M. F. Fontaine, and G. J. Adriaenssens, J. Non-Cryst. Solids **299-302**, 953 (2002).
[16] M. Aniya, J. Non-Cryst. Solids **198-200**, 762 (1996).
[17] J. Li and D. A. Drabold, Phys. Rev. B **61**, 11998 (2000).
[18] J. Li and D. A. Drabold, Phys. Rev. Lett. **85**, 2785 (2000).
[19] F. Shimojo, K. Hoshino, and Y. Zempo, J. Non-Cryst. Solids **312-314**, 388 (2002).
[20] S. I. Simdyankin, S. R. Elliott, Z. Hajnal, T. A. Niehaus, and Th. Frauenheim, Phys. Rev. B **69**, 144202 (2004).
[21] S. I. Simdyankin, T. A. Niehaus, G. Natarajan, Th. Frauenheim, and S. R. Elliott, Phys. Rev. Lett. **94**, 086401 (2005).
[22] S. I. Simdyankin, M. Elstner, T. A. Niehaus, Th. Frauenheim, and S. R. Elliott, Phys. Rev. B **72**, 020202 (2005).
[23] J. Singh and I. K. Oh, J. Non-Cryst. Solids **351**, 1582 (2005).
[24] M. Aniya and F. Shimojo, J. Non-Cryst. Solids **352**, 1510 (2006).
[25] I. Watanabe, Y. Inagaki, and T. Shimizu, J. Phys. Soc. Jpn. **41**, 2030 (1976).
[26] K. S. Liang, A. Bienenstock, and C. W. Bates, Phys. Rev. B **10**, 1528 (1974).
[27] S. Neov, M. Baeva, I. Gerassimova, and M. Nikiforova, Phys. Status Solidi B **57**, 795 (1980).
[28] M. M. Radwan, Chemtronics **4**, 99 (1989).
[29] J. P. Perdew, K. Burke, and M. Ernzerhof, Phys. Rev. Lett. **77**, 3865 (1996).
[30] F. Shimojo, R. K. Kalia, A. Nakano, and P. Vashishta, Comput. Phys. Commun. **140**, 303 (2001).
[31] T. A. Arias, M. C. Payne, and J. D. Joannopoulos, Phys. Rev. B **45**, 1538 (1992).
[32] G. Kresse and J. Hafner, Phys. Rev. B **49**, 14251 (1994).
[33] D. Vanderbilt, Phys. Rev. B **41**, 7892 (1990).
[34] M. Tuckerman, B. J. Berne, and G. J. Martyna, J. Chem. Phys. **97**, 1990 (1992).
[35] G. J. Adriaenssens, A. Gheorghiu-de La Rocque, E. Belin-Ferré, and P. Hertogen, J. Non-Cryst. Solids **266-269**, 898 (2000).
[36] F. Shimojo, M. Aniya, and K. Hoshino, J. Phys. Soc. Jpn. **73**, 2148 (2004).
[37] J. Z. Liu and P. C. Taylor, Phys. Rev. B **41**, 3163 (1990).
[38] F. Shimojo, K. Hoshino, and Y. Zempo, J. Phys. Soc. Jpn. **74**, 621

(2005).
[39] F. Shimojo, K. Hoshino, and Y. Zempo, J. Phys. Soc. Jpn. **72**, 2822 (2003).
[40] M. Itoh, J. Non-Cryst. Solids **210**, 178 (1997).
[41] R. S. Mulliken, J. Chem. Phys. **23**, 1833 (1955).
[42] R. S. Mulliken, J. Chem. Phys. **23**, 1841 (1955).
[43] D. Sánchez-Portal, E. Artacho, and J. M. Soler, J. Phys.: Condens. Matter **8**, 3859 (1996).
[44] M. D. Segall, R. Shah, C. J. Pickard, and M. C. Payne, Phys. Rev. B **54**, 16317 (1996).